DOI: 10.1002/ejic.201100359

A New Series of Nanoporous Ionic Crystals Based on Polyoxometalates – Synthesis, Crystal Structures, and Adsorption Properties

Xiaohui Han,[a] Lin Xu,*[a] Fengyan Li,[a] and Ning Jiang[a]

Keywords: Polyoxometalates / Adsorption / Microporous materials / Ionic crystals / Channel structures

Based on polyoxometalate cluster anions and macrocations, $KH_2[Cr_3O(OOCCH_3)_6(H_2O)_3][\alpha\text{-}GeMo_{12}O_{40}]\cdot 10H_2O$ (**1**), $K_{1.5}H_{1.5}[Cr_3O(OOCCH_3)_6(H_2O)_3][\alpha\text{-}GeW_{12}O_{40}]\cdot 9.5H_2O$ (**2**), $NaH_2[Cr_3O(OOCCH_3)_6(H_2O)_3]_3[\alpha\text{-}P_2W_{18}O_{62}]\cdot 32H_2O$ (**3**), and $Na_3[Cr_3O(OOCCH_3)_6(H_2O)_3]_3[\alpha\text{-}As_2W_{18}O_{62}]\cdot 34H_2O$ (**4**) have been prepared by a conventional method and characterized by single-crystal X-ray diffraction, IR and UV/Vis spectroscopy, elemental analysis, thermogravimetric analysis (TGA) and powder X-ray diffraction (PXRD). In addition, the gas adsorption properties of these four compounds for methanol and ethanol have been investigated. The adsorption studies display an apparent difference between methanol and ethanol vapor adsorption and demonstrate that such microporous materials could be applied as new molecular sieves for selective sorption from a mixture of C_1 and C_2 alcohols.

Introduction

In recent years, much attention has been paid to the fabrication of inorganic or organic–inorganic hybrid nanoporous materials. Due to the well-defined pores and shape- or size-selective adsorption, such materials can be widely applied to adsorption, separation, and heterogeneous catalysis.[1]

Polyoxometalates (POMs), a fascinating class of transition metal oxide cluster anions with unique physical and chemical properties, have potential applications in diverse fields including magnetism, catalysis, materials science, photochemistry, medicine, and chemical analysis.[2] Furthermore, POMs in nanosize structures are suitable inorganic building blocks to form multidimensional and microstructured compounds by rational combination with other inorganic or organic components. Therefore, the development of POM-based solid state materials with various functional properties has received attention.[3] In particular, the design and preparation of POM-based microporous materials similar to zeolites are of considerable significance for application as efficient catalysts.

Recently, Kwon and coworkers reported a combination of POM cluster anions with large aluminium oxo cluster cations to produce ionic crystals with some new features including a nanocomposite nature, porous structure, and sorption properties.[4] Mizuno's group subsequently published their work on the synthesis, structure, and selective sorption/catalysis properties of nanoporous compounds constructed from the interaction of POMs with macrocations.[5] In addition, we have reported analogous ionic crystals based on a large trinuclear chromium cluster, $[Cr_3O(CH_3COO)_6(H_2O)_3]^+$, and investigated their geometric framework and supermolecular architecture by employing various building blocks with different molecular sizes, symmetries, and anion charges.[6] Izarova et al. reported similar compounds by choosing simple inorganic salts of Fe(III) and POMs as reactants,[7] although further studies on the properties of these compounds have not been conducted. Kortz's group has also synthesized this type of solid state material using $[Ru_3O(OOCCH_3)_6(CH_3OH)_3]^+$ as a macrocation.[8] Little work has been conducted to investigate the effect of larger Keggin- and Wells–Dawson-type polyanions on the ionic crystal architecture, though the ionic crystals of larger polyanions may lead to unusual nanosized channels with new adsorption properties. To date, there has been only one report of ionic crystals with a Dawson-type polyanion.[5d]

Herein, we present the synthesis and characterization of four porous ionic crystals based on the $[Cr_3O(CH_3COO)_6(H_2O)_3]^+$ macrocation and Keggin- and Wells–Dawson-type polyanions, $KH_2[Cr_3O(OOCCH_3)_6(H_2O)_3][\alpha\text{-}GeMo_{12}O_{40}]\cdot 10H_2O$ (**1**), $K_{1.5}H_{1.5}[Cr_3O(OOCCH_3)_6(H_2O)_3][\alpha\text{-}GeW_{12}O_{40}]\cdot 9.5H_2O$ (**2**), $NaH_2[Cr_3O(OOCCH_3)_6(H_2O)_3]_3[\alpha\text{-}P_2W_{18}O_{62}]\cdot 32H_2O$ (**3**), and $Na_3[Cr_3O(OOCCH_3)_6(H_2O)_3]_3[\alpha\text{-}As_2W_{18}O_{62}]\cdot 34H_2O$ (**4**). In addition to the introduction of larger Wells–Dawson-type polyanions, we are also interested in the ionic size effect between $[\alpha\text{-}GeMo_{12}O_{40}]^{4-}$ and $[\alpha\text{-}GeW_{12}O_{40}]^{4-}$. Interestingly, **1**–**4** can selectively adsorb methanol molecules with a high uptake between C_1 and C_2 alcohols, disregarding of the size of the polyanion.

[a] Key Laboratory of Polyoxometalates Science of Ministry of Education, College of Chemistry, Northeast Normal University,
Changchun 130024, P. R. China
E-mail: linxu@nenu.edu.cn

Supporting information for this article is available on the WWW under http://dx.doi.org/10.1002/ejic.201100359.

Results and Discussion

Synthesis

Compounds **1**–**4** were all synthesized by a conventional method in acidic aqueous solution. The main change to the synthetic procedure, is that an acetate buffer was selected as the medium for the preparation of **2** and **4**. Moreover, unlike compounds **1**, **3**, and **4**, which were prepared using the plenary Keggin, $[\alpha\text{-}GeMo_{12}O_{40}]^{4-}$, or Wells–Dawson polyanions, $[\alpha\text{-}P_2W_{18}O_{62}]^{6-}$ and $[\alpha\text{-}As_2W_{18}O_{62}]^{6-}$, **2** was synthesized using the trivacant Keggin-type polyanion $[\alpha\text{-}GeW_9O_{34}]^{10-}$ precursor and the lacunary polyanions transformed into the plenary species in the acetate buffer system. This indicates that such porous ionic crystals can also exist at pH value of 4.8 in addition to the pH of 2.0 reported in the literature.[5a–5d,7]

Structure Description

Compounds **1**–**2** and **3**–**4** are isostructural, respectively. The basic packing profiles and the pore characteristics are identical. Herein, we describe the structures of **1** and **3** as representative examples. The structure of **1** is composed of a $[\alpha\text{-}GeMo_{12}O_{40}]^{4-}$ polyanion, $[Cr_3O(OOCCH_3)_6(H_2O)_3]^+$ macrocation, K^+ cation, and crystallization water molecules. The $[\alpha\text{-}GeMo_{12}O_{40}]^{4-}$ anion retains its original α-Keggin structure, with a central GeO_4 tetrahedron surrounded by four Mo_3O_{13} units consisting of edge-sharing MoO_6 octahedra. The bond valance sum calculation suggests that all Mo atoms are in the +6 oxidation state with an average value of 6.110 and all O atoms are in the –2 oxidation state with an average value of –1.902. It indicates that all O atoms within the polyoxoanions are not protonated. The macrocation $[Cr_3O(OOCCH_3)_6(H_2O)_3]^+$ is a trinuclear μ_3-oxobridging complex containing an equilateral triangle of chromium atoms with an oxygen atom at the center, six edge-bridging propanoate groups, and three equatorial aqua ligands.[9] As **1** was formed from acidic aqueous solution, two protons are attached to isolated water molecules to compensate for the charge balance. As shown in Figure 1, the K^+ ion has a eight-coordinate envi-

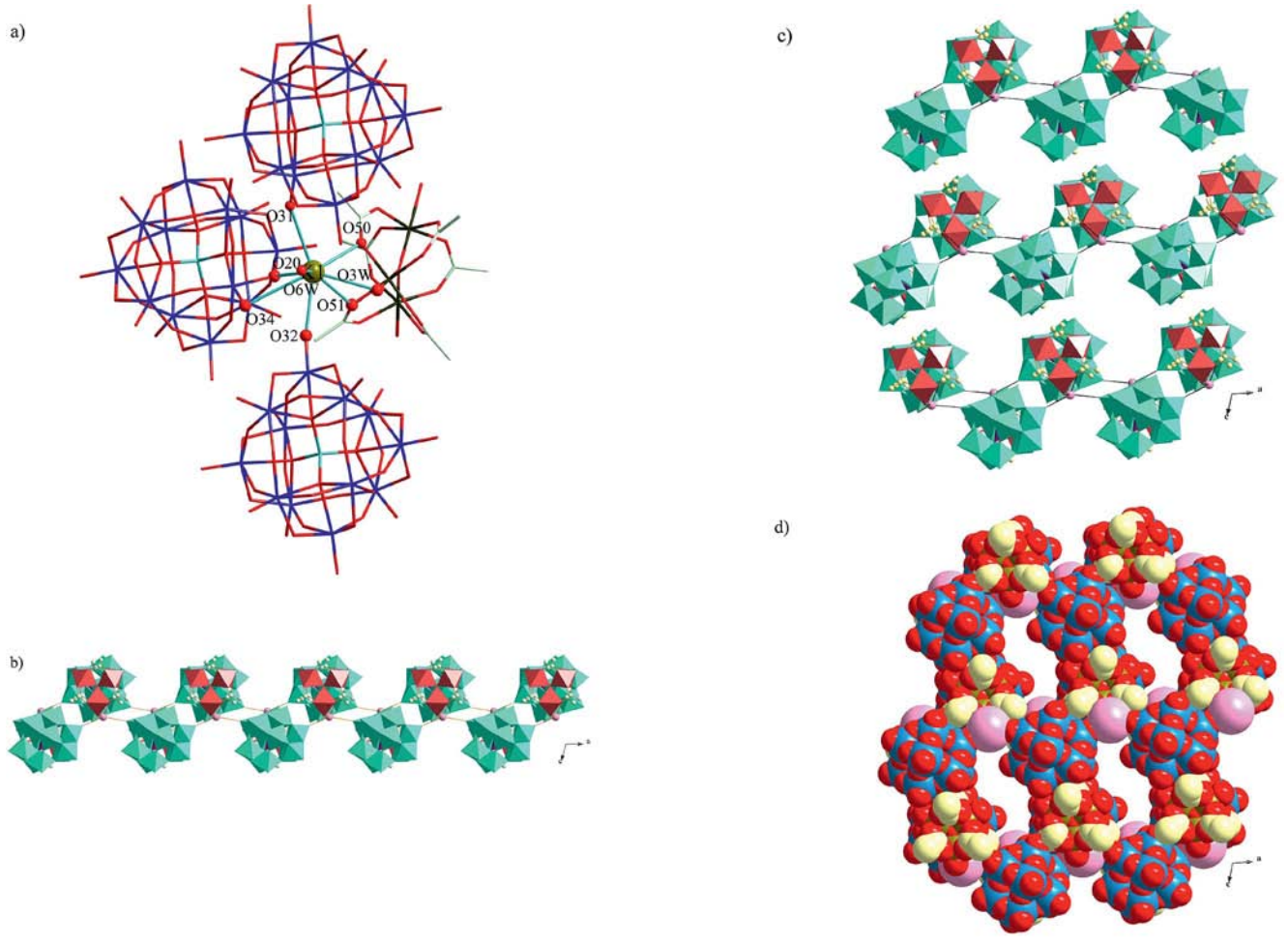

Figure 1. Detailed illustration of the crystal structure of **1**. (a) Coordination environment of the K^+ ion. (b) A view of double-layer zigzag chain along the *b* axis. (c) Combined polyhedral/ball and stick representation of **1** viewed along the *b* axis showing the hexagonal honeycomb. Aquamarine octahedra: MoO_6, purple tetrahedra: GeO_4, salmon octahedra: CrO_6, light pink balls: K atoms, light yellow balls: C atoms. (d) Space-filling representation of **1** consisting of straight channels. Dark blue balls: Mo atoms, yellow-green balls: Cr atoms, red balls: O atoms, light pink balls: K atoms, light yellow balls: C atoms. Lattice water molecules and hydrogen atoms are omitted for clarity.

ronment, coordinated to four oxygen atoms from three polyanions and three oxygen atoms from one macrocation and one water molecule. The K···O distances are 2.665–3.273 Å. As shown in Figure 1 (b), oppositely charged inorganic cluster ions linked by K^+ form a double-layer zigzag chain along the a axis, and the two neighboring 1D chains lead to the formation of a 2D hexagonal honeycomb in the *ac* plane. Seen along the *b* axis, the packing of the 2D hexagonal honeycomb sheets generate a straight 1D channel with an accessible dimension of about 15.6×5.6 Å^2 (see Figure 1, c). These channels are occupied by water molecules, which are coordinated to K^+ ions or hydrogen-bonded (O_W···O 2.549–3.032 Å) to the oxygen atoms of the POMs or macrocations in the vicinity. Multiple hydrogen bonds as well as electrostatic interactions exist between the neighboring layers.

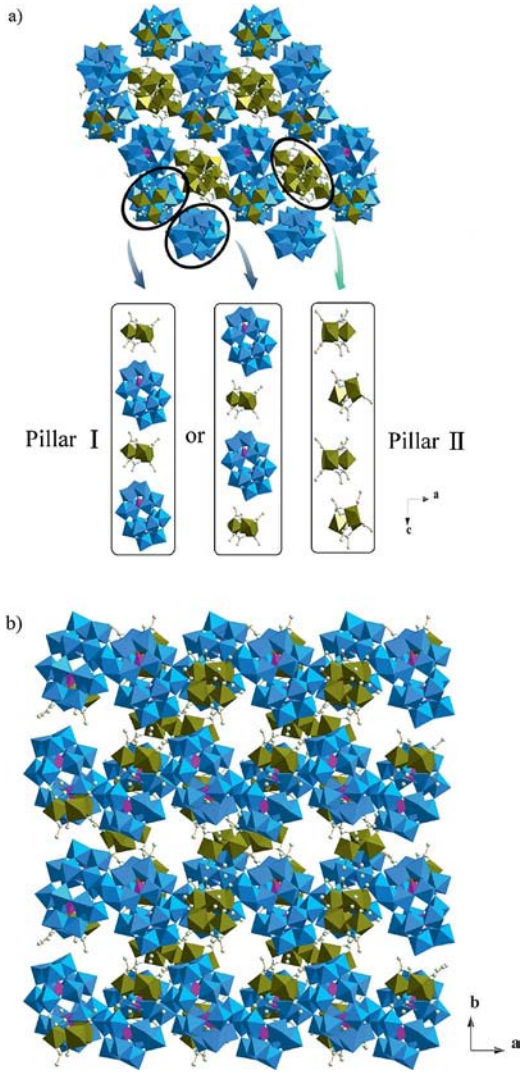

Figure 2. Crystal structures of **3**. Lattice water molecules, hydrogen, and Na atoms are omitted for clarity. (a) Ball and stick/polyhedral representation viewed along the *b* axis (b) ball and stick/polyhedral representation viewed along the *c* axis. Dark blue octahedra: WO_6, deep pink tetrahedra: PO_4, yellow-green octahedra: CrO_6, light green balls: C atoms.

The structure of **3** consists of a $[\alpha\text{-}P_2W_{18}O_{62}]^{6-}$ anion, $[Cr_3O(OOCCH_3)_6(H_2O)_3]^+$ macrocation, Na^+ cation, and crystallization water molecules. As **3** was formed from acidic aqueous solution, two protons are attached to isolated water molecules to compensate for the charge balance. Unlike the structures of **1** and **2**, two types of pillars can be noticed in the structure of **3**: Dawson-type polyanions and macrocations arrayed alternately along the *b* axis to constitute pillar I, and macrocations constitute pillar II. As shown in Figure 2 (a), six parallel I pillars stack next to each other to generate a straight hexagonal honeycomb-like 1D channel, which forms a cavity for pillar II. In addition, each of the hexagonal honeycomb-like channel of I pillars alternates with polyanions and macrocations. Lattice water molecules occupy the residual space and form hydrogen bonds with the oxygen atoms of the POMs and macrocations in the vicinity (O_W···O = 2.436–3.01 Å). As shown in Figure 2 (b) another type of channel is observed along the *c* axis. In **1**–**4**, oppositely charged cluster ions self-assembled by coordination of K^+/Na^+ ions, electrostatic interactions, and hydrogen bonds to form a new 3D framework. The compounds with channels can offer potential adsorption properties.

UV/Vis Spectroscopy

The electronic properties of **2** and **4** were investigated in the range 200–800 nm. In the UV absorption spectrum of **2**, the band with a maximum at around 265 nm assigned to the $O_{b(c)}$–W charge transition is observed, which is characteristic for Keggin-type POM anions. In the UV absorption spectrum of **4**, two bands at around 240 and 310 nm are assigned to O_d–W and $O_{b(c)}$–W charge transfer transitions, respectively. In the visible region, both **2** and **4** exhibit two bands at 439 and 582 nm which can be ascribed to $^4A_{2g} \rightarrow {}^4T_{1g}$ and $^4A_{2g} \rightarrow {}^4T_{2g}$ d–d transitions of Cr^{3+} in the macrocation, respectively (Figures S5–S8).

Thermal Analysis

The thermal stabilities of **1**–**4** were determined by TGA. The TG curve of **1** exhibits four weight loss steps (Figure S9). The first weight loss of 4.95% in the temperature range of 25–181.3 °C corresponds to the removal of 7.5 crystallization water molecules (calcd. 5.06%). The second weight loss of 1.68% between 181.3–203.5 °C is attributed to the loss of 2.5 crystallization water molecules (calcd. 1.7%). The third weight loss of 1.9% in the range of 203.5–315 °C is ascribed to the release of the three water ligands of the macrocation (calcd. 2.02%). Further weight loss occurs around 315–472 °C, which is due to the loss of six propanoate ligands from the macrocation. Above 472 °C, complete decomposition of **1** occurs forming mixed metal oxides. The total weight loss (20.83%) agrees with the calculated value (21.07%).

TGA performed on **2** shows three weight loss steps (as shown in Figure S10). In the range of 47–325 °C, consecu-

tive two step weight losses observed with a total weight loss of 5.9% are due to the loss of 9.5 crystallization water molecules and three coordinated water molecules of the macrocation (calcd. 6.1%). The last weight loss of 8.7% from 325 to 595 °C is ascribed to the release of six propanoate ligands from the macrocation (calcd. 9.5%). The total weight loss (14.6%) agrees with the calculated value (15.6%).

The TGA plot of **3** shows two weight loss steps (as shown in Figure S11). The first weight loss is 11.2% at 45.6–287.4 °C, corresponding to the loss of 32 crystallization water molecules and nine coordinated water molecules from the macrocation (calcd. 11.1%). The second stage, which occurs from 287.4 to 500 °C, is attributed to the loss of 18 propanoate ligands from the macrocation (calcd. 15.8%). The observed weight loss (24.4%) is in agreement with the calculated value (26.9%).

In the TG curve of **4** (as shown in Figure S12), a weight loss of 11.2% occurs at around 22.7–283.4 °C, corresponding to the consecutive loss of 34 crystallization water molecules and nine coordinated water molecules from the macrocation (calcd. 11.3%). The subsequent weight loss of 12.9% from 283.4 to 482 °C is attributed to the release of 18 propanoate ligands from the macrocation (calcd. 15.5%). Above 567.5 °C, the framework of the polyoxoanion decomposed gradually. The total weight loss (24.1%) is close to the calculated value (26.8%).

Sorption Studies

The methanol and ethanol adsorption isotherms of **1a**–**4a** at 298 K were investigated to quantify the adsorption properties. P and P_0 are the vapor pressure of the adsorbate in adsorption measurements and the saturated vapor pressure of the adsorbate, respectively, and P/P_0 denotes the relative pressure of the adsorbate.

As shown by Mizuno for this class of nanoporous materials, the amount of guest molecule adsorption is inversely proportional to the number of carbon atoms and the charges of polyanions.[10] In this paper, the amount of alcohol uptake of **1a**–**4a** is also inversely proportional to the increase of the number of carbon atoms in agreement with Mizuno. In addition, these polyanions (Keggin- or Wells–Dawson-type) selected for our work have the same charge, so the relationship of the adsorption properties with the charges of polyanions was not established.

As shown in Figure 3, the value of methanol uptake of **1a** increased with an increase in P/P_0 and reached approximately 5.11 wt.-% at $P/P_0 = 0.72$. The slope became steeper above this point and the uptake reached approximately 12.87 wt.-% at $P/P_0 = 0.96$. Whereas, the isotherm for ethanol showed plateaus and the value of ethanol uptake adsorption was only 1.14 wt.-% at $P/P_0 = 0.95$.

The results of methanol and ethanol adsorption isotherms for **2a** at 298 K were analogous to that of **1a**. For the adsorption curve in Figure 4, the amount of methanol uptake increased monotonically with P/P_0 and reached approximately 8.08 wt.-% at $P/P_0 = 0.97$. On the other hand,

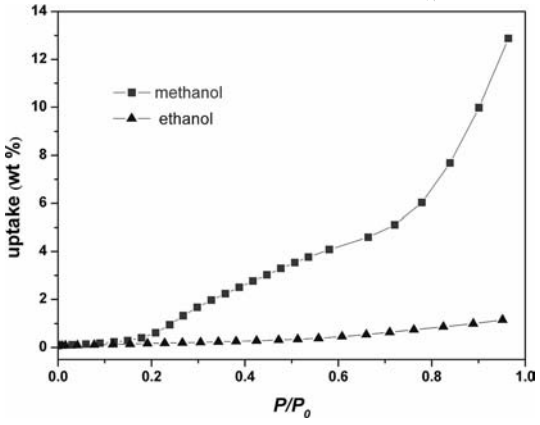

Figure 3. Adsorption isotherms of methanol and ethanol at 298 K with **1a**.

the amount of ethanol uptake adsorption was 0.45 wt.-% even if the P/P_0 value approached 0.95, which was negligible compared to the methanol uptake.

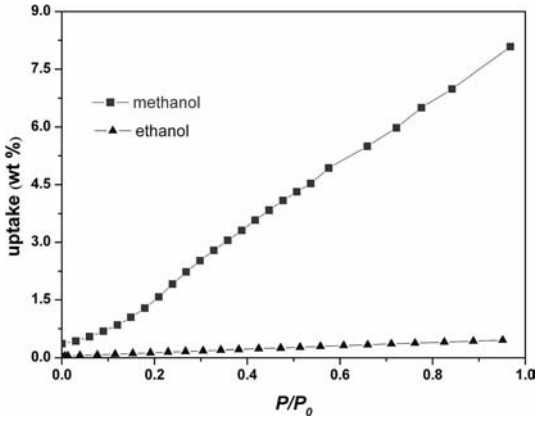

Figure 4. Adsorption isotherms of methanol and ethanol at 298 K with **2a**.

Figure 5 shows the methanol and ethanol adsorption isotherms of **3a** at 298 K. Steep methanol uptakes were observed in the isotherms at low relative pressure (P/P_0 = 0.15); subsequently, the amount of sorption increased with

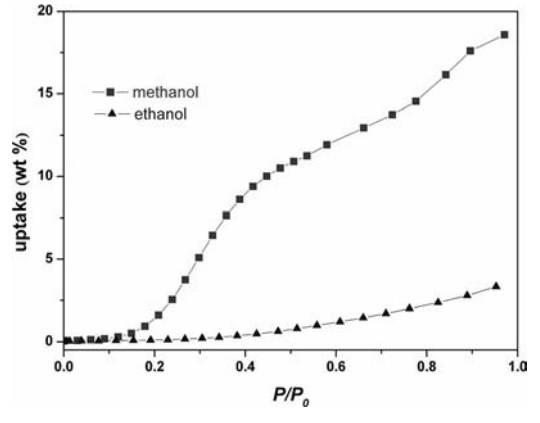

Figure 5. Adsorption isotherms of methanol and ethanol at 298 K with **3a**.

the increase in the vapor pressure and achieved approximately 18.59 wt.-% at P/P_0 = 0.97. For ethanol, the isotherm showed almost a plateau and the value of uptake adsorption was only 3.32 wt.-% at P/P_0 = 0.95.

Figure 6 shows the adsorption isotherms of **4a**. It is similar to that of **3a** with 16.21 wt.-% methanol uptake at P/P_0 = 0.97 and 2.47 wt.-% ethanol uptake at P/P_0 = 0.96, respectively.

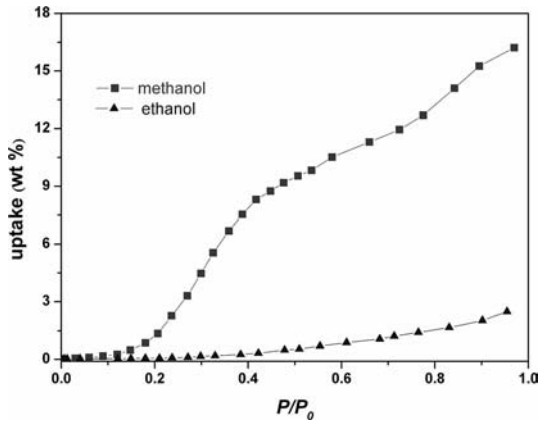

Figure 6. Adsorption isotherms of methanol and ethanol at 298 K with **4a**.

According to the adsorption studies above, we find obviously different adsorption isotherms between methanol and ethanol for **1a**–**4a** even if the difference between the methanol and ethanol molecules is only one methyl group. This demonstrates that guest inclusions of **1a**–**4a** can selectively adsorb methanol molecules with a high uptake between C_1 and C_2 alcohols. These distinctive guest inclusion properties do not change whether Keggin (**1a**–**2a**) or Dawson (**3a**–**4a**) type POM anions are the building blocks.

To further investigate the influence of the anion clusters over methanol adsorption uptake, comparisons between **1a**–**2a** and **3a**–**4a** were studied, respectively.

As shown in Figure 7, both the values of methanol uptake of **1a**–**2a** increased with an increase in P/P_0 ($P/P_0 <$ 0.78), the slope of methanol adsorption isotherms of **1a** became steeper above P/P_0 = 0.78 and reached approximately 12.87 wt.-% at P/P_0 = 0.96; whereas the sorption branch of **2a** increased monotonically with the same slope and reached 8.08 wt.-% at P/P_0 = 0.97. This shows that when the charges of the POMs and the heteroatom are the same, the difference of W^{VI}/Mo^{VI} in the POMs may affect the methanol adsorption uptake. In addition, both the methanol adsorption isotherms and the amounts of the methanol adsorption uptake for **3a** were nearly the same as that for **4a**. This illustrates that the effect of the heteroatom diversity (P/As) in POMs on methanol adsorption could be negligible. That is to say that the type of POMs (W^{VI} or Mo^{VI}) is another factor related to the amount of the methanol adsorption in addition to the charges of the POMs, the molecular sizes, and dipole moments of guest molecules that have been reported in literature.

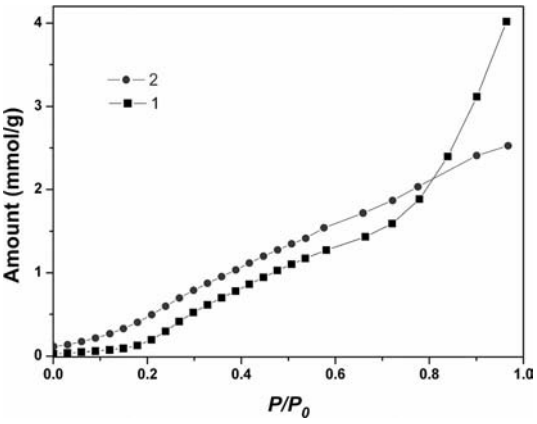

Figure 7. Methanol adsorption isotherms of **1a** and **2a** at 298 K.

Conclusions

In summary, a series of new nanoporous crystals composed of macrocation $[Cr_3O(CH_3COO)_6(H_2O)_3]^+$ and four different POM anion clusters have been synthesized and investigated. The polyanions and macrocations form a framework with nanosized channels through the coordination of K^+/Na^+ ions, electrostatic interactions, and hydrogen bonds. Adsorption studies demonstrate that these microporous materials have potential applications as new molecular sieves for selective sorption from a mixture of C_1 and C_2 alcohols.

Experimental Section

Materials and Methods: All chemicals were reagent grade and used as received without further purification. Distilled water was used throughout. $[Cr_3O(OOCCH_3)_6(H_2O)_3]NO_3{\cdot}nH_2O$ was synthesized and characterized by IR spectroscopy according to the published procedure.[9] H_4-[α-$GeMo_{12}O_{40}$]·nH_2O, K_8Na_2[α-GeW_9O_{34}]·$25H_2O$, H_6[α-$P_2W_{18}O_{62}$]·nH_2O, and Na_6[α-$As_2W_{18}O_{62}$]·nH_2O were all synthesized according to the literature methods[11] and identified by IR spectroscopy. Elemental analyses were performed with a Perkin–Elmer 2400 CHN elemental analyzer; Ge, P, As, Cr, Mo and W were analyzed with a Plasma-Spec (I) ICP atomic emission spectrometer and with a PE-3030 atomic absorption spectrophotometer for K and Na. IR spectra were recorded with an Alpha Centaurt FTIR spectrophotometer in the range of 400–4000 cm^{-1} using KBr pellets. UV/Vis spectra were recorded with an in situ Varian Cary 50 Conc UV/Vis spectrophotometer. TG analysis was conducted with a Perkin–Elmer TGA7 instrument in flowing N_2 with a heating rate of 10 °C/min. PXRD measurements were performed with a Rigaku D/MAX-3 instrument with Cu-K_a radiation in the 2θ range of 3–40° at 298 K.

Vapor Adsorption: The methanol and ethanol vapor adsorption measurements were performed with a Hiden Isochema Intelligent Gravimetric Analyser (IGA-100B). The samples (ca. 100 mg) were evacuated to a constant weight at 323 K (for **1**–**2**) and 353 K (for **3**–**4**) under a high vacuum ($< 10^{-6}$ mbar). The liquid used to generate the vapor was fully degassed by freeze-pump-thaw cycles. The saturated vapor pressures of methanol and ethanol at 298 K were 15.6 and 6.67 KPa, respectively.

Synthesis of Crystals of 1–4

$KH_2[Cr_3O(OOCCH_3)_6(H_2O)_3][\alpha\text{-}GeMo_{12}O_{40}]\cdot 10H_2O$ (1): To distilled water (15 mL) was added $H_4[\alpha\text{-}GeMo_{12}O_{40}]\cdot nH_2O$ (0.37 g, 0.20 mmol). The mixture was stirred at room temperature until $H_4[\alpha\text{-}GeMo_{12}O_{40}]\cdot nH_2O$ was completely dissolved, $[Cr_3O(OOCCH_3)_6(H_2O)_3]NO_3\cdot nH_2O$ (0.15 g, 0.20 mmol) was slowly dissolved in to the reaction mixture, and the obtained green solution was stirred for 40 min. Then KCl (2.5 mL of 1 mol·L^{-1} solution) was added, and the mixture was stirred for 1 h at 303 K. After cooling to room temperature, the solution was filtered into a 50 mL beaker. Slow evaporation of the solvent at room temperature led to green crystals of **1** suitable for X-ray diffraction after 7 d; yield 55%. FTIR (KBr): $\tilde{\nu}$ = 1611.9 [ν_{as} (OCO)], 1454.6 [ν_s (OCO)], 962.8 [ν_{as} (Mo=O_d)], 914.1 [ν_{as} (Mo–O_b–Mo)], 792.7 [ν_{as} (Ge–O_a)], 664.3 [ν_{as} (Cr–O)] cm^{-1}. $C_{12}H_{46}Cr_3GeKMo_{12}O_{66}$ (2665.4): calcd. C 5.41, H 1.74, K 1.47, Cr 5.85, Ge 2.73, Mo 43.19; found C 5.30, H 1.82, K 1.43, Cr 5.77, Ge 2.67, Mo 43.27.

$K_{1.5}H_{1.5}[Cr_3O(OOCCH_3)_6(H_2O)_3][\alpha\text{-}GeW_{12}O_{40}]\cdot 9.5H_2O$ (2): $K_8Na_2[\alpha\text{-}GeW_9O_{34}]\cdot 25H_2O$ (0.62 g, 0.20 mmol) was dissolved in KAc/HAc buffer (15 mL, pH = 4.8) followed by addition of $[Cr_3O(OOCCH_3)_6(H_2O)_3]NO_3\cdot nH_2O$ (0.15 g, 0.20 mmol) and KCl (2.0 mL of 1 mol L^{-1} solution). The mixture was stirred for 40 min at room temperature and for another 1 h at 303 K. After cooling to room temperature, the solution was filtered into a 50 mL beaker. After 10 d green crystals of **2** were isolated by evaporating the solvent slowly at room temperature; yield 70%. FTIR (KBr): $\tilde{\nu}$ = 1609.1 [ν_{as} (OCO)], 1452.5 [ν_s (OCO)], 977.2 [ν_{as} (W=O_d)], 891.4 [ν_{as} (Ge–O_a)], 827.7 [ν_{as} (W–O_b–W)], 779.1 [ν_{as} (W–O_c–W)], 666.5 [ν_{as} (Cr–O)] cm^{-1}. $C_{12}H_{44,5}Cr_3GeK_{1,5}O_{65,5}W_{12}$ (3730.4): calcd. C 3.86, H 1.20, K 1.57, Cr 4.18, Ge 1.94, W 59.14; found C 3.78, H 1.09, K 1.50, Cr 4.07, Ge 1.88, W 59.31.

$NaH_2[Cr_3O(OOCCH_3)_6(H_2O)_3]_3[\alpha\text{-}P_2W_{18}O_{62}]\cdot 32H_2O$ (3): To distilled water (15 mL) was added $H_6[\alpha\text{-}P_2W_{18}O_{62}]\cdot nH_2O$ (0.45 g, 0.10 mmol). The turbid solution was stirred and slightly heated until it was clear. $[Cr_3O(OOCCH_3)_6(H_2O)_3]NO_3\cdot nH_2O$ (0.15 g, 0.2 mmol) and NaCl (2.5 mL of 1 mol L^{-1} solution) were added. After stirring for 1 h at 303 K, the solution was cooled to room temperature, filtered into a 50 mL beaker, and the filtrate was allowed to evaporate slowly at ambient temperature. Green crystals of **3** were obtained after 2 weeks; yield 60%. FTIR (KBr): $\tilde{\nu}$ = 1613.1 [ν_{as} (OCO)], 1454.6 [ν_s (OCO)], 1094.1 [ν_{as} (P–O_a)], 962.7 [ν_{as} (W=O_d)], 914.1 [ν_{as} (W–O_b–W)], 792.9 [ν_{as} (W–O_c–W)], 663.5 [ν_{as} (Cr–O)] cm^{-1}. $C_{36}H_{138}Cr_9NaO_{142}P_2W_{18}$ (6705.6): calcd. C 6.45, H 2.07, Na 0.34, P 0.92, Cr 6.98, W 49.35; found C 6.38, H 2.18, Na 0.30, P 0.99, Cr 7.07, W 50.08.

$Na_3[Cr_3O(OOCCH_3)_6(H_2O)_3]_3[\alpha\text{-}As_2W_{18}O_{62}]\cdot 34H_2O$ (4): To NaAc/HAc buffer (15 mL, pH = 4.8) was added $Na_6[\alpha\text{-}As_2W_{18}O_{62}]\cdot nH_2O$ (0.47 g, 0.10 mmol). The turbid solution was stirred and slightly heated until it was clear. $[Cr_3O(OOCCH_3)_6(H_2O)_3]NO_3\cdot nH_2O$ (0.15 g, 0.2 mmol) and NaCl (2.5 mL of 1 mol L^{-1} solution) were added. After stirring for 1 h at 303 K, the solution was cooled to room temperature, filtered into a 50 mL beaker, and the filtrate was allowed to evaporate slowly at ambient temperature. Green crystals of **4** were obtained after 2 weeks; yield 60%. FTIR (KBr): $\tilde{\nu}$ = 1618.8 [ν_{as} (OCO)], 1454.8 [ν_s (OCO)], 967.0 [ν_{as} (W=O_d)], 900.6 [ν_{as} (W–O_b–W)], 865.9 [ν_{as} (As–O_a)], 775.3 [ν_{as} (W–Oc–W)], 666.7 [ν_{as} (Cr–O)] cm^{-1}. $C_{36}H_{140}As_2Cr_9Na_3O_{144}W_{18}$ (6873.5): calcd. C 6.29, H 2.03, Na 1.00, Cr 6.81, As 2.18, W 48.14; found C 6.38, H 2.10, Na 1.11, Cr 6.92, As 2.09, W 48.31.

X-ray Crystallography: Single-crystal XRD data of compounds **1**–**4** were collected with a Bruker SMART APEX II CCD single-crystal diffractometer using Mo-K_α radiation (λ = 0.71073 Å) at room temperature. All of the structures were solved by direct method using the program SHELXS-97[12] and refined by full-matrix least-squares method on F^2 with the use of the SHELXL-97 software package.[13] Absorption corrections were applied using the multiscan technique. In the final refinements, all the metal atoms and most of the oxygen atoms were refined with anisotropic temperature factors. Hydrogen atoms for water molecules were not determined in the crystal structure refinements. A summary of the crystal data and structure refinement for **1**–**4** are provided in Table S1.

CCDC-808179 (for **1**), -808180 (for **2**), -808181 (for **3**), and -808182 (for **4**) contain the supplementary crystallographic data for this paper. These data can be obtained free of charge from The Cambridge Crystallographic Data Centre via www.ccdc.cam.ac.uk/data_request/cif.

Supporting Information (see footnote on the first page of this article): IR spectra, UV/Vis spectra, TG curves, PXRD data, methanol adsorption isotherms of **1a**–**2a** and **3a**–**4a** at 298 K, a summary of the crystal data and structure refinement for **1**–**4**, and selected distances (≤ 3.1 Å) between the oxygen atoms of the lattice water molecules and the oxygen atoms of POMs and macrocations for **1**–**4**.

Acknowledgments

This work was financially supported by the National Natural Science Foundation of China (NSFC) (grant numbers 20731002, 20971019 and 21001021) and the Fundamental Research Funds for the Central Universities. This work was also supported by the Program for Changjiang Scholars and Innovative Research Team in University.

[1] a) O. M. Yaghi, L. Guangming, L. Hailian, *Nature* **1995**, *378*, 703–706; b) O. M. Yaghi, H. Li, T. L. Groy, *Inorg. Chem.* **1997**, *36*, 4292–4293; c) J. S. Seo, D. Whang, H. Lee, S. I. Jun, J. Oh, Y. J. Jeon, K. Kim, *Nature* **2000**, *404*, 982–986; d) N. Guillou, Q. Gao, P. M. Forster, J. S. Chang, M. Nogue's, S. E. Park, G. Fe'rey, A. K. Cheetham, *Angew. Chem. Int. Ed.* **2001**,*40*, 2831–2834; e) E. J. Cussen, J. B. Claridge, M. J. Rosseinsky, C. J. Kepert, *J. Am. Chem. Soc.* **2002**, *124*, 9574–9581; f) S. Kitagawa, R. Kitaura, S. Noro, *Angew. Chem. Int. Ed.* **2004**, *43*, 2334–2375; g) C. Y. Sun, S. X. Liu, D. D. Liang, K. Z. Shao, Y. H. Ren, Z. M. Su, *J. Am. Chem. Soc.* **2009**, *131*, 1883–1888.

[2] a) M. T. Pope, A. Müller, *Angew. Chem. Int. Ed. Engl.* **1991**, *30*, 34–*48*; b) *Polyoxometalate Chemistry: From Topology via Self-Assembly to Applications* (Eds.: M. T. Pope, A. Müller), Kluwer, Dordrecht, The Netherlands, **2001**; c) *Polyoxometalate Chemistry for Nano-Composite Design* (Eds.: T. Yamase, M. T. Pope), Kluwer, Dordrecht, The Netherlands, **2002**; d) *Polyoxometalate Molecular Science* (Eds.: J. J. Borr-as-Almenar, E. Coronado, A. Müller, M. T. Pope), Kluwer, Dordrecht, The Netherlands, **2004**; e) P. Mialane, C. Duboc, J. Marrot, E. Rivière, A. Dolbecq, F. Sécheresse, *Chem. Eur. J.* **2006**, *12*, 1950–1959; f) M. J. Manos, A. J. Tasiopoulos, E. J. Tolis, N. Lalioti, J. D. Woollins, A. Z. Slawin, M. P. Sigalas, T. A. Kabanos, *Chem. Eur. J.* **2003**, *9*, 695–703; g) U. Kortz, A. Müller, J. van Slageren, J. Schnack, N. S. Dalal, M. Dressel, *Coord. Chem. Rev.* **2009**, *253*, 2315–2327; h) A. Dolbecq, E. Dumas, C. R. Mayer, P. Mialane, *Chem. Rev.* **2010**, 110,6009–6048; i) C. L. Hill, *J. Mol. Catal. A* **2007**, *262*, 2–6; j) C. Boglio, G. Lemière, B. Hasenknopf, S. Thorimbert, E. Lacôte, M. Malacria, *Angew. Chem. Int. Ed.* **2006**, *45*, 3324–3327; k) D. Kumar, E. Derat, A. M. Khenkin, R. Neumann, S. Shaik, *J. Am. Chem. Soc.* **2005**, *127*, 17712–17718; l) A. Müller, S. Roy, *Coord. Chem. Rev.* **2003**, *245*, 153–166; m) T. Ruether, V. M. Hultgren, B. P.

Timko, A. M. Bond, W. R. Jackson, A. G. Wedd, *J. Am. Chem. Soc.* **2003**, *125*, 10133–10143; n) T. Liu, *J. Am. Chem. Soc.* **2003**, *125*, 312–313; o) B. B. Xu, Z. H. Peng, Y. G. Wei, D. R. Powell, *Chem. Commun.* **2003**, 2562–2563.

[3] a) B. J. S. Johnson, S. A. Geers, W. W. Brennessel, V. G. Young, *Dalton Trans.* **2003**, *24*, 4678–4681; b) J. M. Knaust, C. Inman, S. W. Keller, *Chem. Commun.* **2004**, *5*, 492–493; c) F. Hussain, B. S. Bassil, L. H. Bi, M. Reicke, U. Kortz, *Angew. Chem. Int. Ed.* **2004**, *43*, 3485–3488; d) E. Coronado, C. Giménez-Saiz, C. J. Gómez-García, S. C. Capelli, *Angew. Chem. Int. Ed.* **2004**, *43*, 3022–3025; e) A. Müller, D. Rehder, E. T. K. Haupt, A. Merca, H. Bögge, M. Schmidtmann, H. Brückner, *Angew. Chem. Int. Ed.* **2004**, *43*, 4466–4470; f) C. P. Pradeep, M. F. Misdrahi, F. Y. Li, J. Zhang, L. Xu, D. L. Long, T. B. Liu, L. Cronin, *Angew. Chem. Int. Ed.* **2009**, *48*, 8309–8313; g) C. H. Li, K. L. Huang, Y. N. Chi, X. Liu, Z. G. Han, L. Shen, C. W. Hu, *Inorg. Chem.* **2009**, *48*, 2010–2017; h) W. L. Queen, S.-J. Hwu, S. Reighard, *Inorg. Chem.* **2010**, *49*, 1316–1318; i) D. L. Long, R. Tsunashima, L. Cronin, *Angew. Chem. Int. Ed.* **2010**, *49*, 1736–1758; j) S. Z. Li, P. T. Ma, J. P. Wang, Y. Y. Guo, H. Z. Niu, J. W. Zhao, J. Y. Niu, *CrystEngComm* **2010**, *12*, 1718–1721.

[4] a) J. H. Son, H. Choi, Y.-U. Kwon, *J. Am. Chem. Soc.* **2000**, *122*, 7432–7433; b) J. H. Son, Y.-U. Kwon, *Inorg. Chem.* **2003**, *42*, 4153–4159; c) J. H. Son, Y.-U. Kwon, *Inorg. Chem.* **2004**, *43*, 1929–1932.

[5] a) S. Uchida, M. Hashimoto, N. Mizuno, *Angew. Chem. Int. Ed.* **2002**, *41*, 2814–2817; b) S. Uchida, N. Mizuno, *Chem. Eur. J.* **2003**, *9*, 5850–5857; c) S. Uchida, N. Mizuno, *J. Am. Chem. Soc.* **2004**, *126*, 1602–1603; d) S. Uchida, R. Kawamoto, T. Akatsuka, S. Hikichi, N. Mizuno, *Chem. Mater.* **2005**, *17*, 1367–1375; e) R. Kawamoto, S. Uchida, N. Mizuno, *J. Am. Chem. Soc.* **2005**, *127*, 10560–10567; f) S. Uchida, R. Kawamoto, N. Mizuno, *Inorg. Chem.* **2006**, *45*, 5136–5144; g) A. Lesbani, R. Kawamoto, S. Uchida, N. Mizuno, *Inorg. Chem.* **2008**, *47*, 3349–3357; h) S. Uchida, R. Kawamoto, H. Tagami, Y. Nakagawa, N. Mizuno, *J. Am. Chem. Soc.* **2008**, *130*, 12370–12376; i) S. Uchida, H. Tagami, N. Mizuno, *Angew. Chem. Int. Ed.* **2009**, *48*, 6160–6164.

[6] X. S. Qu, L. Xu, Y. F. Qiu, G. G. Gao, F. Y. Li, Y. Y. Yang, *Z. Anorg. Allg. Chem.* **2007**, *633*, 1040–1047.

[7] a) N. V. Izarova, M. N. Sokolov, A. V. Virovets, *Russ. J. Inorg. Chem.* **2004**, *49*, 690–693; b) N. V. Izarova, M. N. Sokolov, A. V. Virovets, H. G. Platas, V. P. Fedin, *J. Struct. Chem.* **2005**, *46*, 1147–153.

[8] M. Ibrahim, M. H. Dickman, A. Suchopar, U. Kortz, *Inorg. Chem.* **2009**, *48*, 1649–1654.

[9] F. A. Cotton, W. N. Wang, *Inorg. Chem.* **1982**, *21*, 2675–2678.

[10] S. Uchida, N. Mizuno, *Coord. Chem. Rev.* **2007**, *251*, 2537–2546.

[11] a) R. D. Claude, F. Michel, F. Raymonde, *Inorg. Chem.* **1983**, *22*, 207–216; b) L. H. Bi, U. Kortz, S. Nellutla, A. C. Stowe, J. van Tol, N. S. Dalal, B. Keita, L. Nadjo, *Inorg. Chem.* **2005**, *44*, 896–903; c) R. G. Finke, M. W. Droege, P. J. Domaille, *Inorg. Chem.* **1987**, *26*, 3886–3896; d) R. Acerete, C. F. Hammer, L. C. W. Baker, *Inorg. Chem.* **1984**, *23*, 1478–1482.

[12] G. M. Sheldrick, *SHELXS97*, *Program for Crystal Structure Refinement*, University of Göttingen, Germany, **1997**.

[13] G. M. Sheldrick, *SHELXS97*, *Program for Crystal Structure Solution*, University of Göttingen, Germany, **1997**.

Received: April 5, 2011
Published Online: September 2, 1022

